Malaysian Journal of Chemistry, 2025, Vol. 27(1), 265-273
(Special Issue: *International Conference in Organic Synthesis, ICOS 2024*)

Synthesis of Titanium Dioxide Microspheres via a Modified Hydrothermal Method Utilizing Schott Bottle and Improvised Clamp

Musa, M. Z.[1,2]*, Subki, A. S. R. A.[5], Malek, M. F.[3], Parimon, N.[6], Hassan, H.[4] and Mamat, M. H.[2]

[1]Electrical Engineering Studies, College of Engineering, Universiti Teknologi MARA Cawangan Pulau Pinang, 13500 Permatang Pauh, Pulau Pinang, Malaysia

[2]NANO-ElecTronic Centre (NET), College of Engineering, Universiti Teknologi MARA, 40450 Shah Alam, Selangor, Malaysia

[3]NANO-SciTech Laboratory, Centre for Functional Materials and Nanotechnology, Institute of Science (IOS), Universiti Teknologi MARA, 40450 Shah Alam, Selangor, Malaysia

[4]Chemical Engineering Studies, College of Engineering, Universiti Teknologi MARA Cawangan Pulau Pinang, 13500 Permatang Pauh, Pulau Pinang, Malaysia

[5]Faculty of Electrical and Electronics Engineering Technology, Universiti Teknikal Malaysia Melaka, Hang Tuah Jaya, 76100 Durian Tunggal, Melaka, Malaysia

[6]Centre of Research in Energy and Advanced Materials (CREAM), Faculty of Engineering, Universiti Malaysia Sabah, Jalan UMS, 88400 Kota Kinabalu, Sabah, Malaysia

*Corresponding author (e-mail: musa_zahidi59@uitm.edu.my)

A synthesis of titanium dioxide (TiO_2) microspheres has been realized via a facile hydrothermal method utilizing glass bottle and stainless-steel clamp. The unique structure has been produced after 4 hours of deposition time at the temperature of 150°C. The resulting samples were analysed using FESEM, XRD, Raman spectroscopy, XPS, and humidity sensing measurement. FESEM images revealed the TiO_2 microspheres shape with the average diameter of 5 µm, are constructed of smaller dendritic TiO_2 nanorods. XRD analysis confirmed that the TiO_2 is of a rutile structure with preferred orientation at (110), and (101) plane. Raman vibration mode was detected at 143 cm^{-1}, 235 cm^{-1}, 447 cm^{-1}, and 612 cm^{-1}, which correspond to B_{1g} and two-phonon bands E_g and A_{1g}, respectively. It is expected that the projected ultra-high surface area of the structure can be advantageous for various applications.

Keywords: Titanium dioxide; microspheres; tantalum doping; humidity sensor

Received: September 2024; Accepted: December 2024

As a semiconductor material, TiO_2 has been gathering interest due to its various beneficial properties. It is a very chemically stable material with high photocatalytic property and wide bandgap energy while also being non-toxic. The demand for this compound stemmed from its' successful application as photocatalysts [1], photoanode in solar cells [2, 3], antibacterial coatings [4], and various types of sensors [5].

In an effort to further expand the potential of TiO_2, there have been many endeavors by researchers to synthesis nanostructured TiO_2. For example, Pathinti et al. [6] have produced nanorod-shape TiO_2 via hydrothermal method with 3.41 µm length and average diameter of 239 nm. They have managed utilized the structure to improve the ethanol sensing performance of a cholesteric liquid crystal. In another work, Yang et al. [7] have successfully produced sphere-shaped TiO_2 which consisted of nanocone monomer also by using hydrothermal method. The increased surface area of the resultant TiO_2 have been instrumental in increasing the photocatalytic degradation of tetracycline. Utilizing electrochemical anodization, Motola et al. [8] have synthesized TiO_2 nanotubes with a thickness of ~5 mm and average inner diameter of ~250 nm. This top-down approach of producing TiO_2 nanostructure requires high-voltage potentiostat and chemical etching.

Most of the work on the synthesis of TiO_2 microspheres required the use of autoclave as the vessel for the growth of TiO_2 crystal. This apparatus is known to be bulky and having a very thick metal wall. As a result, longer time is usually needed to heat the solution inside. Consequently, the growth of the TiO_2 crystal using autoclave is relatively slow with duration exceeding 10 hours is quite common as reported by many researchers [9-14]. To the best of our knowledge, there has not been any report on the synthesis of TiO_2 microsphere using a simple modified hydrothermal method utilizing glass bottle as the vessel. In this work, a home-made clamp was utilized to ensure the pressure inside the glass bottle increased to enable the growth of TiO_2 crystal. $TaCl_5$ were often used as the Ta dopant

†Paper presented at the International Conference in Organic Synthesis 2024 (ICOS 2024)

source in producing Ta-doped TiO_2 [15-17]. In this work, the addition of $TaCl_5$ as the dopant source have been shown to contribute to the formation of microsphere by increasing the acidity of the solution.

EXPERIMENTAL

Chemicals and Materials

Chemicals were used as received (from Sigma-Aldrich and Merck) without further purification. Titanium butoxide $Ti(C_4H_9O)_4$ as a precursor for TiO_2 was purchased from Sigma Aldrich with 97% purity. Hydrochloric acid (HCl) 37% was obtained from Merck. The doping source, $TaCl_5$ 99.8% purity, was also purchased from Merck. Finally, deionized (DI) water was used as part of the solution.

Sample Preparation

Microscope glass slide was chosen as the substrate. The slide was cut into 2 cm × 2 cm size using diamond cutter before being cleaned ultrasonically with acetone, methanol, and deionized (DI) water in that sequence in an ultrasonic bath (Hwasin Technology PowerSonic 405, 40 kHz). The substrates were then blow-dried using nitrogen gas and were kept in airtight container to avoid contamination before being used for deposition later on.

The substrates were deposited with a thin layer of TiO_2 seed layer using RF magnetron sputtering (SNTEK), which is a physical vapour deposition (PVD) method. High purity TiO_2 target (99.99% purity) was used as the source with deposition power of 200 W. Plasma was generated using argon (Ar) gas at the flow of 20 sccm while 5 sccm of oxygen (O_2) gas was also added for complete reaction. The chamber pressure was controlled at 5 mTorr during deposition through automated adjustable butterfly valve. The duration of deposition time was 6 hours to reach average thickness of 370 nm.

A solution immersion method was employed to produce TiO_2 nanostructure. The immersion solution was prepared by first mixing deionised (DI) water and hydrochloric acid (HCl) at 1:1 ratio in a Schott bottle and was stirred for 10 min. Then, appropriate amount of tetrabutyl titanate, $Ti(C_4H_9O)_4$ (97%, Sigma-Aldrich) was added to the solution as Ti precursor to achieve a concentration of 0.07 M. For the Ta-doped sample, $TaCl_5$ was added to the solution to achieved 3 at. % doping concentration. The solution was then stirred for another 50 min. Glass substrate coated with TiO_2 seed layer was inserted into the solution with the seed layer facing upward. To ensure that no solution was lost during heating and pressure build up inside the bottle, the bottle was tightly closed using high heat resistance cap. The bottle was then clamped using home-made clamp as shown in Figure 1. Then, the solution was heated in a furnace at 150°C for 4 hours before the sample was removed and thoroughly rinsed using DI water. Finally, the sample was annealed at 400°C in an oven.

Figure 1. Photo image of Schott bottle sealed with home-made clamp.

Characterization Methods

The morphology of the TiO_2 microspheres was characterized using field emission scanning electron microscope (FESEM; model: JEOL JSM-7600F). The structural properties of the samples were examined using x-ray diffractometer (XRD; Shimadzu XRD-6000, Japan, Cu-Kα radiation, wavelength of 0.154 nm) and Raman spectroscopy (Horiba Jobin Yvon-79DU420A-OE-325, France, 514 nm Ar laser). X-ray photoelectron spectroscopy (XPS, Thermo Scientific Nexsa G2, USA) analysis of the samples was also conducted to determine the samples' chemical states. The survey scan was done using pass energies of 280 eV while the narrow scan used pass energy of 112 eV.

To assess the performance of the prepared samples for application as humidity sensor, Ag metal contact have been deposited on the TiO_2 film using thermal evaporator (ULVAC Thermal Evaporator, Japan). The current value between two metal contact was measured using two-point probe and source measurement unit (SMU, Keithley 2400) under changing humidity environment (40-90%RH) inside a humidity chamber (ESPEC-SH261, Japan). The sensitivity value, S was calculated using the following equation [18]:

$$S = \frac{R_{40}}{R_{90}}$$

RESULTS AND DISCUSSION

Structural Properties

FESEM image of the resulting undoped and Ta-doped TiO_2 is shown in Figure 2. The undoped TiO_2 sample shown in Figure 2 (a) and (b) exhibits a flower-like structure. The flower consisted of TiO_2 nanorod with diameter of around 100 nm. In contrast, Ta-doped TiO_2 shown in Figure 2 (c) and (d) represent a clear sphere-shaped morphology with average diameter of 5 µm. A higher magnification image reveals that the microsphere consisted of dendritic closely packed nanorods with average diameter of 10 nm.

There are several chemical reactions involved in the formation of TiO_2 crystals. The hydrolysis reaction occurs involving the TiO_2 precursor, H_2O and HCl:

$$Ti(OCH_2CH_2CH_2CH_3)_4 + 4H_2O \xrightarrow{HCl} Ti(OH)_4 + 4ROH$$

$$Ti(OH)_4 \rightarrow TiO_2 + 2H_2O$$

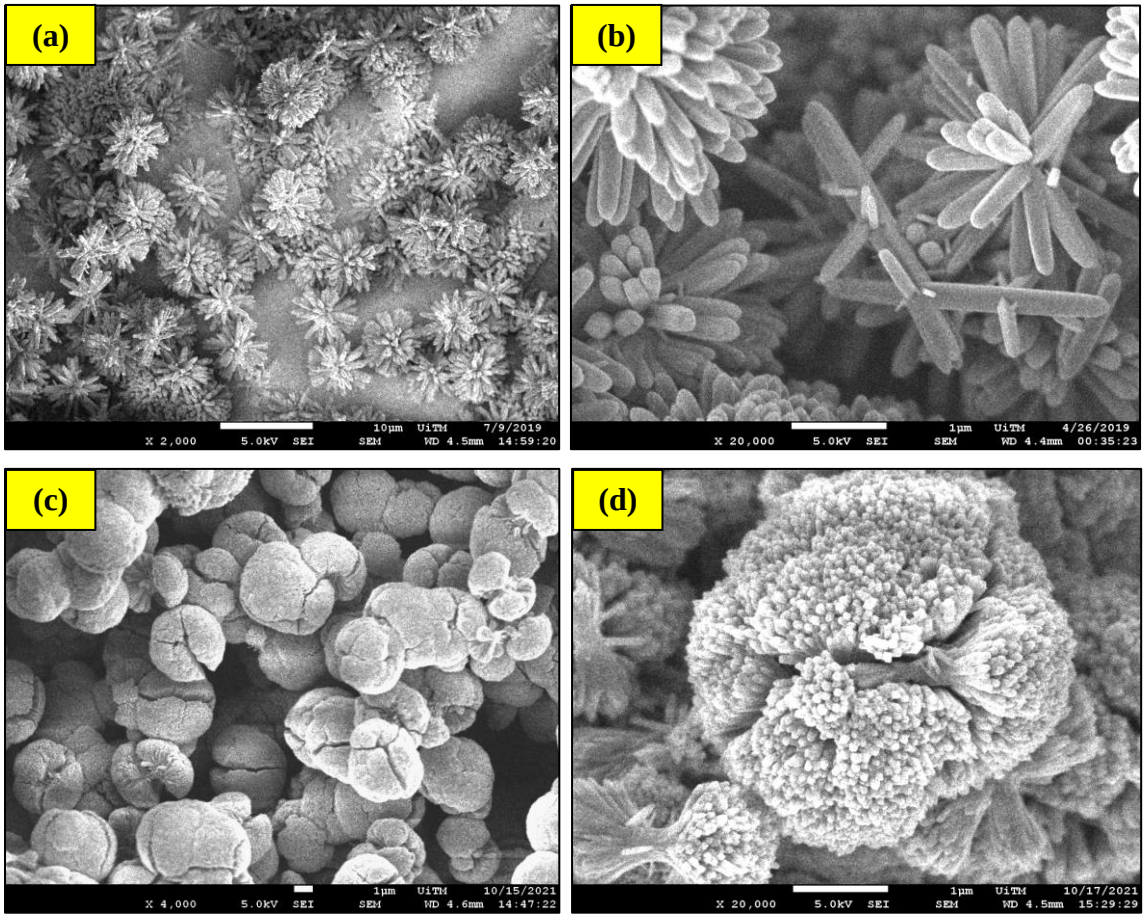

Figure 2. FESEM images of the undoped ((a) and (b)) and Ta-doped TiO_2 ((c) and (d)).

where, $R = C_4H_9$. The reaction produced titanium hydroxyl by removing four carbon atoms from the titanium butoxide. Dehydration or condensation immediately followed generating TiO_2 and water. The addition of HCl was important to stabilize the reactions thus avoiding the creation of large aggregates. In the titanium starting material, tetrabutyl titanate and highly electronegative OR^- ligands shared the titanium's four valence electrons in the equatorial hybrid orbitals, leaving the two axial orbitals vacant. When water was added, a hydrolysis reaction occurred, replacing the OR^- ligands with nucleophilic OH^- (hydroxo) groups derived from the dissociation of H_2O. In the other hand, the OR^- ligand was protonated to form ROH (alcohol). The empty axial orbitals then acquired an electron pair from water molecules to form a neutral hydroxo-aquo $[Ti(OH)_4(OH_2)_2]^0$ complex. These neutral complexes typically aggregate into amorphous TiO_2 because of the van der Waals forces. Nonetheless, the supplement of HCl mitigated this issue. The acid decreased the concentration of dissociated hydroxide ions $[OH^-]$ in the solution and protonated OH^- ligands in the Ti-hydroxo complex, that enhanced electrostatic repulsion between the complexes and thwarted their immediate condensation. Under highly acidic conditions and supersaturation, interconnected three-dimensional TiO_2 structure could be formed. The summary of the reaction mechanism is presented in Figure 3.

In the case of Ta-doped TiO_2, it is believed that the addition of $TaCl_5$ as a dopant source has increased the acidity of the solution thus favouring the formation of densely packed nanorod to form TiO_2 microsphere. Cl^- ions are reported to contribute to deprotonation of the cation due to their high electronegativity, which intensely attracts protons [19]. The increased amount of Cl^- ions in the $TaCl_5$ added solution suggest increased deprotonation reaction leading to formation of TiO_6 octahedra in radial direction [20]. As a result, a microsphere structure of TiO_2 have been realised.

XRD spectra of the synthesized material is depicted in Figure 4. Prominent peaks were observed at 2θ of 27°, 36°, and 54° which correspond to (110), (101), and (211) plane respectively. The sharp and high intensity peaks suggest good crystallinity of the material. According to JCPDS 25-0922, this suggested both of the samples are of a rutile TiO_2 structure. In addition, the Ta-doped TiO_2 sample also exhibited a peak at 25° which relates to (001) plane based on JCPDS No. 25-0922. The overall peak intensity also appears to decrease slightly for the Ta-doped sample. This is a common phenomenon for doped materials since the addition of foreign atoms usually disrupts the crystallinity of TiO_2 due to the difference in atomic radius between the dopant and the parent atom [21, 22]. Overall, both of the sample exhibited good crystal growth based on the XRD peak intensity which is comparable to the work by other researchers using chemical vapour deposition (CVD) [23] or conventional hydrothermal method [24]. This suggested that the home-made clamp have succeeded in replicating the pressure required for the growth of TiO_2 crystal. This type of apparatus is a viable substitution for the more expensive and bulky autoclaves.

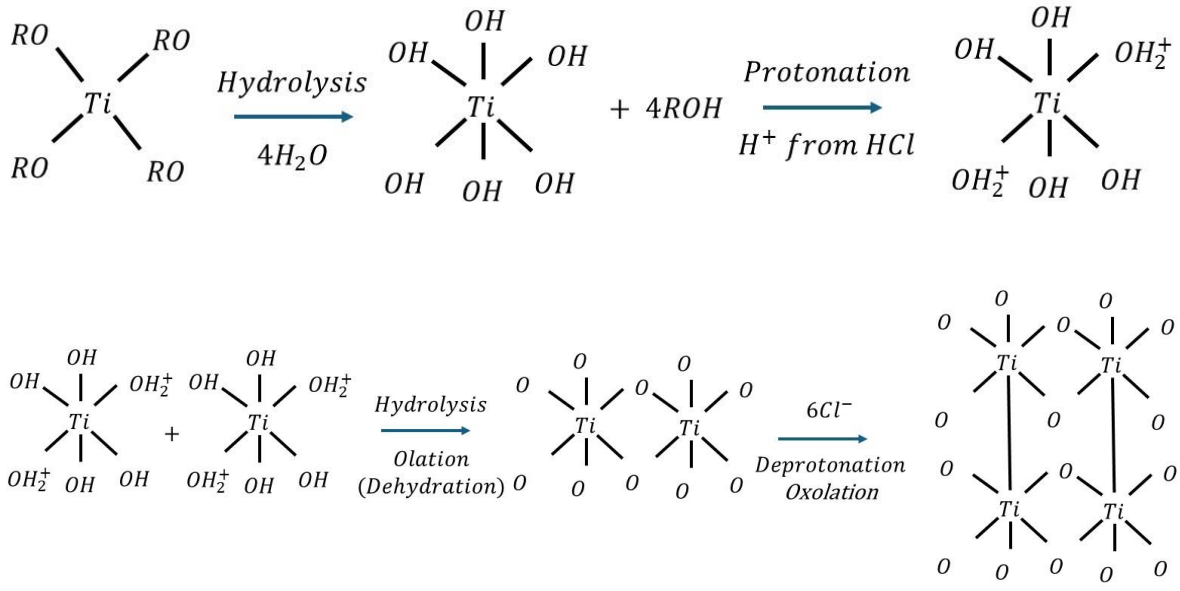

Figure 3. Summary of the reaction during formation of TiO_2 compound.

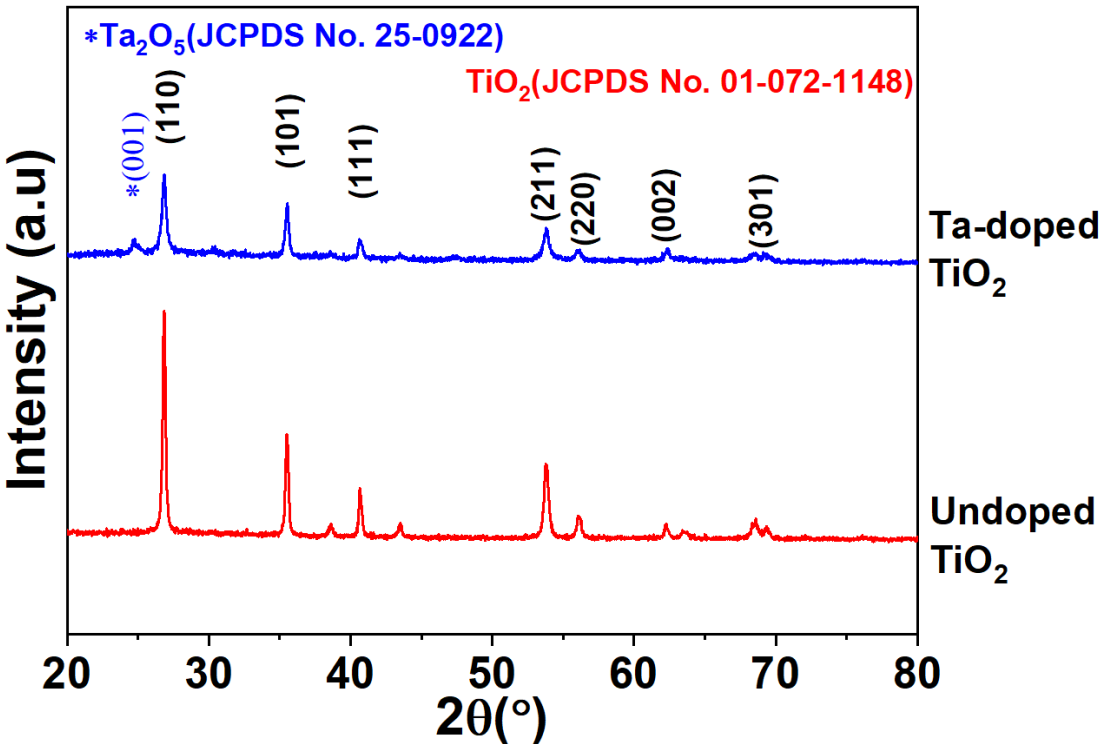

Figure 4. XRD spectra of the undoped and Ta-doped TiO_2.

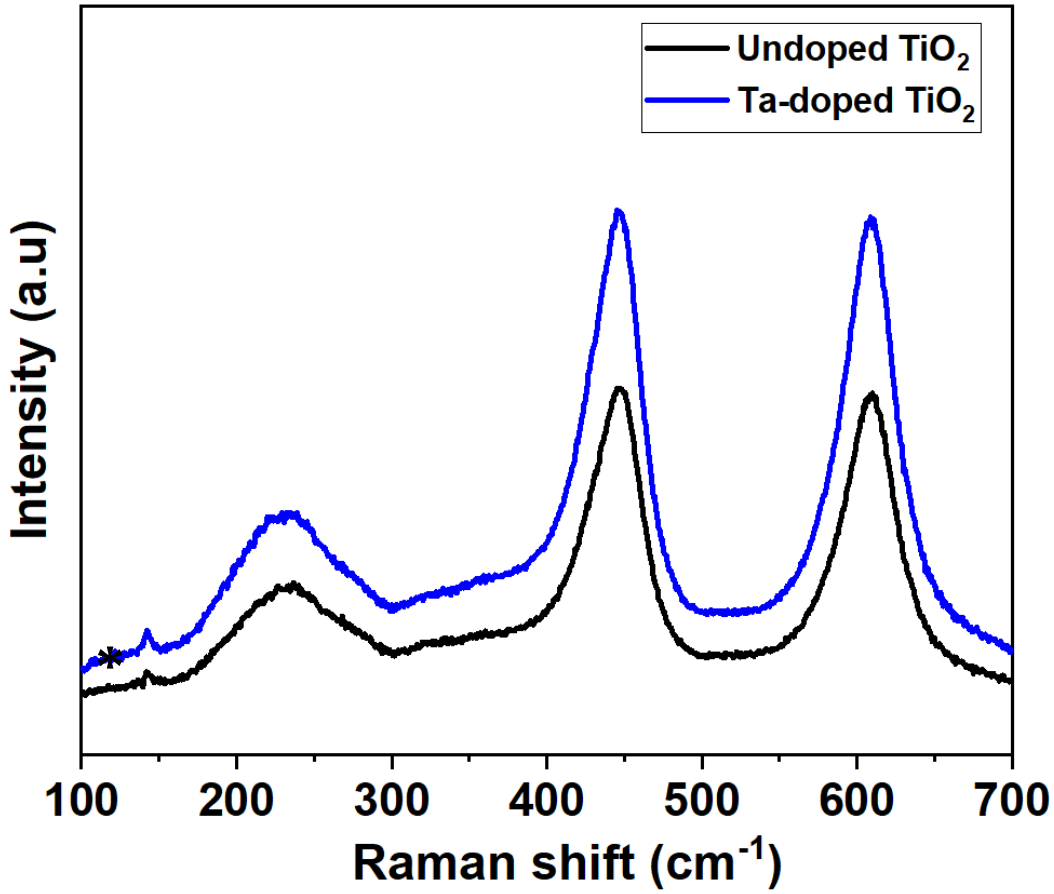

Figure 5. Raman spectra of the undoped and Ta-doped TiO_2.

Raman spectra of the prepared samples are shown in Figure 5. Raman active modes were detected at 143, 235, 447 and 612 cm^{-1} which correspond to B_{1g}, two-phonon bands (marked with *), E_g and A_{1g} respectively. These peaks suggest a rutile structure of TiO_2, without the presence of anatase and brookite phases, which is in line with the XRD results. The A_{1g} peak relates to the vibration modes of the released oxygen atoms from the phase along the c-axis. Meanwhile, the E_g peak represents the vibration modes of Ti-O stretch.

Chemical State Analysis

XPS analysis result of the Ta-doped TiO_2 microsphere is shown in Figure 6. The scan survey in Figure 6 (a) affirms the presence of Ti, O, and Ta elements in the sample. The core-level scan of Ti shown in Figure 6 (b) unveiled two peaks of $2p_{3/2}$ and $2p_{1/2}$ pointing to Ti^{4+} oxidation state. The narrow scan of O 1s depicted in Figure 6 (c) exhibits peak at 529.5 eV which is ascribed to O-Ti bond and broader peak at 532 eV attributed to presence of the hydroxyl group (OH) [25]. The latter peak also indicates the presence of oxygen vacancy on the structure surface which is often considered beneficial with regard to increasing water affinity for humidity sensor application.

Humidity Sensing Properties

The Ta-doped TiO_2 microspheres have been tested for humidity sensing characteristics by fabricating a metal-semiconductor-metal (MSM) resistive-type humidity sensor. The measurement setup for humidity sensor is depicted in Figure 7. The measurement was done inside a humidity-controlled chamber. Figure 8 depicted the result of the current response to the changes in relative humidity for the undoped and Ta-doped TiO_2 microsphere. It is evidenced from the graph that Ta-doped TiO_2 microsphere has shown higher sensitivity to relative humidity compared to the undoped TiO_2. The sensitivity was calculated to increase to 632 for Ta-doped TiO_2 microsphere compared to 196 for the undoped TiO_2. This is most probably due to the increased surface area possessed by the Ta-doped TiO_2 microsphere structure.

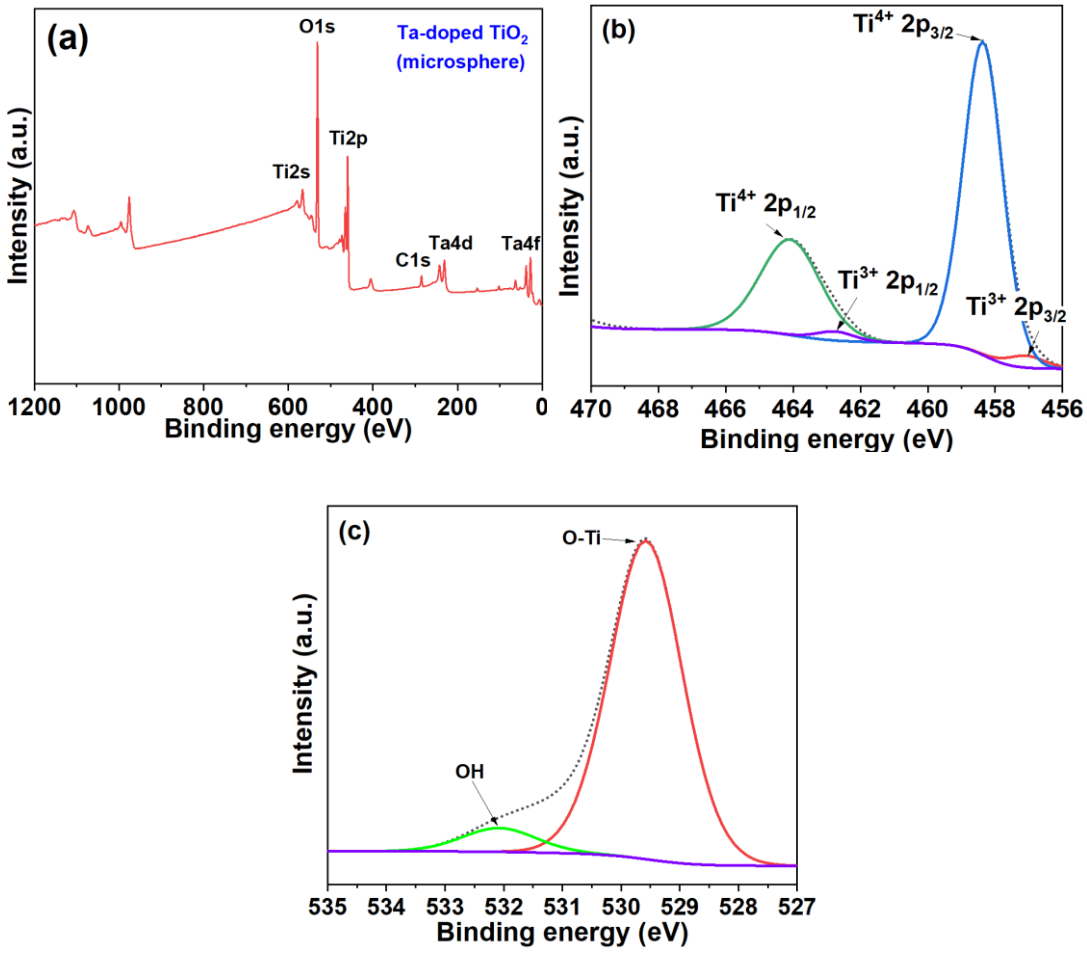

Figure 6. (a) XPS survey scan of TiO_2 microsphere, (b) Ti 2p scan of TiO_2 microsphere, and (c) O 1s scan of TiO_2 microsphere.

As shown by the FESEM images in Figure 2, the reduction in the nanorod diameter for the Ta-doped TiO_2 microsphere sample would likely have resulted in the increase in surface area as reported by Tian et al. [26]. The humidity detection mechanism of a resistive-type humidity sensor is often being related to the of amount of water adsorption on the material surface [27]. When water molecules are absorbed to the TiO_2 surface, the electrical resistance of TiO_2 is reduced. Since the TiO_2 microsphere has been shown to have larger surface area, humidity detection is found to be more sensitive.

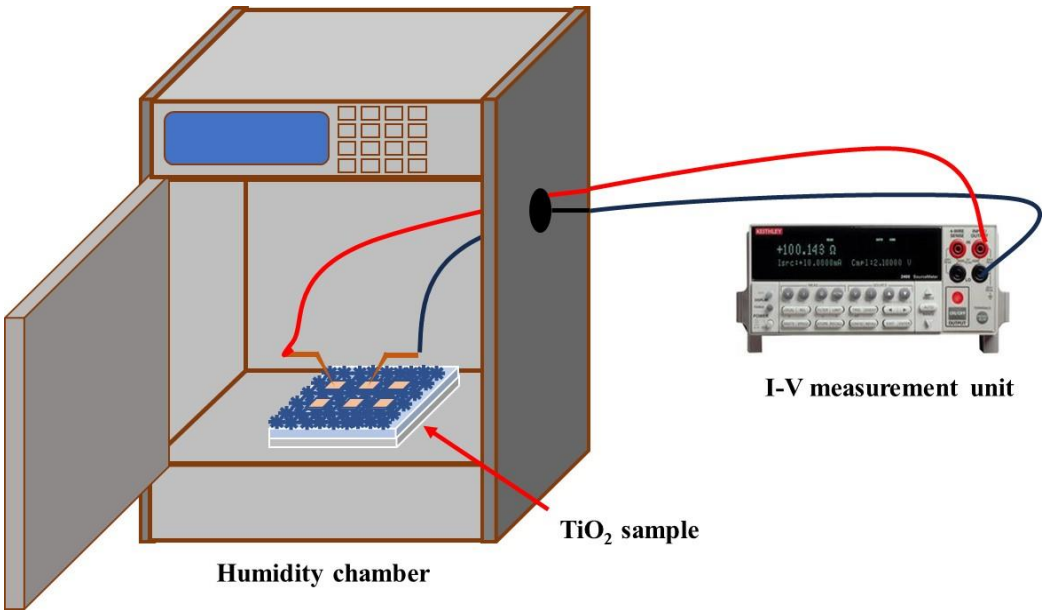

Figure 7. Humidity sensing measurement setup.

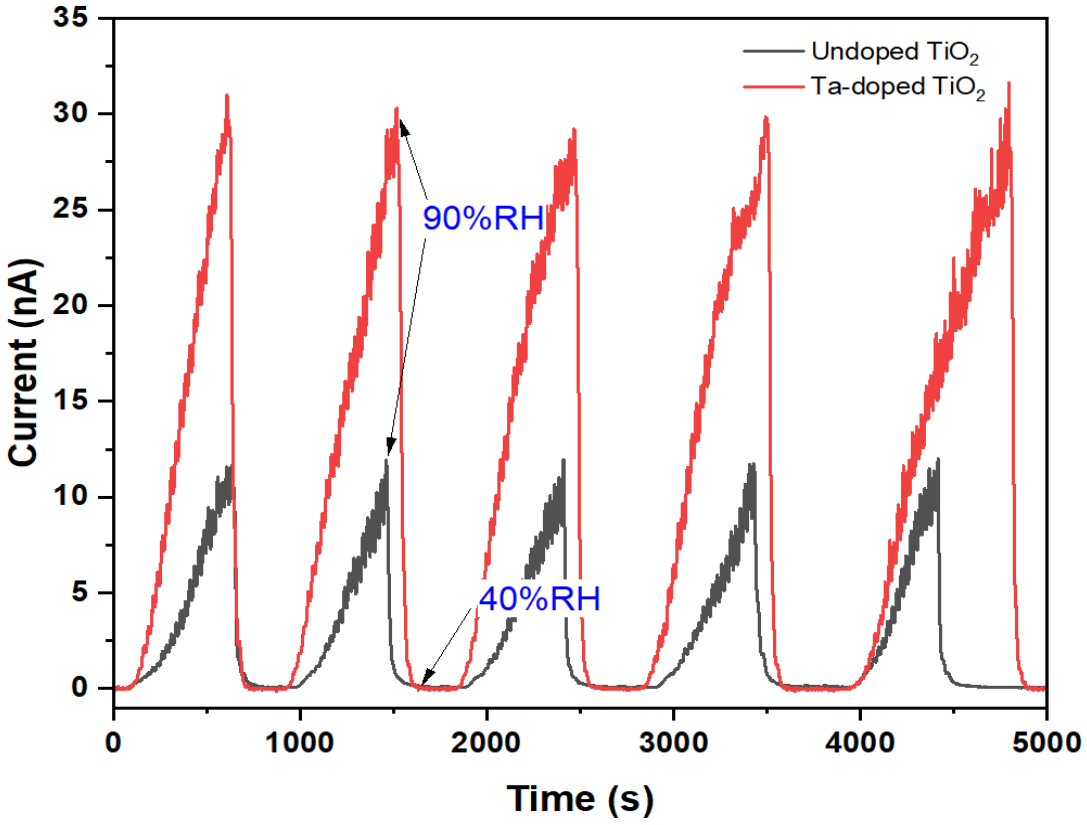

Figure 8. Current measurement at different humidity value of the prepared samples.

CONCLUSION

In this work, a modified hydrothermal method has been utilized to produce TiO_2 microspheres. The structure has been grown in a glass bottle, sealed using an improvised clamp. The clamp has managed to provide the pressure similar to autoclave which enabled the growth of TiO_2 crystal. The addition of $TaCl_5$ has transformed the TiO_2 structure from a flower-like to sphere-shaped architecture. The sample has good crystallinity with an extremely large surface area. Humidity sensor fabricated using the TiO_2 microsphere was shown to have higher sensitivity attributed to the higher surface area which would have facilitated more efficient water adsorption.

ACKNOWLEDGEMENTS

The author acknowledges Research Management Unit (RMU), UiTM Cawangan Pulau Pinang for the support in the completion of this work.

REFERENCES

1. Tashkandi, N. Y., Albukhari, S. M. and Ismail, A. A. (2022) Mesoporous TiO_2 enhanced by anchoring Mn_3O_4 for highly efficient photocatalyst toward photo-oxidation of ciprofloxacin. *Optical Materials*, **127**, 112274.

2. Bakr, Z. H., Wali, Q., Ismail, J., Elumalai, N. K., Uddin, A. and Jose, R. (2018) Synergistic combination of electronic and electrical properties of SnO_2 and TiO_2 in a single SnO_2-TiO_2 composite nanofiber for dye-sensitized solar cells. *Electrochimica Acta*, **263**, 524–532.

3. Hazim Khir, A. K. P., Muhammad Shakeel Ahmad, Nasrudin Abd Rahim and Buddhi, D. (2024) Enhanced Charge Transfer of TiO2 Photoanode for Low Temperature Dye Sensitized Solar Cell via Tin Sintering Aid Integration. *Malaysian Journal of Chemistry*, **26(3)**, 73–80.

4. Singh, J., Hegde, P. B., Avasthi, S. and Sen, P. (2022) Scalable Hybrid Antibacterial Surfaces: TiO_2 Nanoparticles with Black Silicon. *ACS Omega*, **7(9)**, 7816–7824.

5. Mohamed Zahidi, M., et al. (2022) Evaluating Different TiO_2 Nanoflower-Based Composites for Humidity Detection. *Sensors*, **22(15)**, 5794.

6. Pathinti, R. S., Dasari, S. G., Gollapelli, B., Gogula, S., R. R. M. V. and Vallamkondu, J. (2024) Enhanced ethanol gas detection using TiO_2 nanorods dispersed in cholesteric liquid crystal: Synthesis, characterization, and sensing performance. *Journal of Alloys and Compounds*, **994**, 174731.

7. Yang, W. and Bu, Q. (2024) Microsphere structure enhances the photocatalytic performance of TiO_2-CdS heterojunction. *Materials Letters*, **367**, 136619.

8. Motola, M., Hromadko, L., Prikryl, J., Sopha, H., Krbal, M. and Macak, J. M. (2020) Intrinsic properties of high-aspect ratio single- and double-wall anodic TiO_2 nanotube layers annealed at different temperatures. *Electrochimica Acta*, **352**, 136479.

9. Liu, B. and Aydil, E. S. (2009) Growth of Oriented Single-Crystalline Rutile TiO_2 Nanorods on Transparent Conducting Substrates for Dye-Sensitized Solar Cells. *Journal of the American Chemical Society*, **131(11)**, 3985–3990.

10. Ben Naceur, J., Jrad, F., Souiwa, K., Ben Rhouma, F. and Chtourou, R. (2021) Hydrothermal reaction time effect in wettability and photoelectrochemical properties of TiO_2 nanorods arrays films. *Optik*, **239**, 166794.

11. Daneshvare Asl, S., Eslami Saed, A. and Sadrnezhaad, S. K. (2019) Hierarchical rutile/anatase TiO_2 nanorod/nanoflower thin film: Synthesis and characterizations. *Materials Science in Semiconductor Processing*, **93**, 252–259.

12. Takci, D. K. (2021) Synthesis, characterization and dielectric properties of rutile TiO_2 nano-flowers. *Journal of Crystal Growth*, **578**, 126442.

13. Santhi, K., Navaneethan, M., Harish, S., Ponnusamy, S. and Muthamizhchelvan, C. (2020) Synthesis and characterization of TiO_2 nanorods by hydrothermal method with different pH conditions and their photocatalytic activity. *Applied Surface Science*, **500**, 144058.

14. Shinde, P. V., Gagare, S., Rout, C. S. and Late, D. J. (2020) TiO_2 nanoflowers based humidity sensor and cytotoxic activity. *RSC Advances*, **10(49)**, 29378–29384.

15. Paul, R. K. K. and P. S. (2023) Tantalum doped titanium dioxide nanoparticles for efficient photocatalytic degradation of dyes. *Journal of Molecular Structure*, **1277**, 134869.

16. Sun, X. -Y., Liu, C., Chen, Z. and Ma, Y. -Q. (2018) The photocatalytic performance of Ta and Rh co-doped TiO_2 tuned by the average dopant valence. *Materials Research Bulletin*, **100**, 153–160.

17. Meng, Q., Liu, B., Liu, H., Cai, Y. and Dong, L. (2018) Effects of S and Ta codoping on

photocatalytic activity of rutile TiO_2. *Journal of Sol-Gel Science and Technology*, **86(3)**, 631-639.

18. Lin, W. -D., Lin, Y. -C., Wu, R. -J. and Chavali, M. (2021) Gr/3D-ZnO Nanocomposites as Humidity Sensors with Enhanced Sensing Response. *Polymers*, **13(10)**, 1623.

19. Prathan, A., et al. (2020) Controlled Structure and Growth Mechanism behind Hydrothermal Growth of TiO_2 Nanorods. *Scientific Reports*, **10(1)**, 8065.

20. Jordan, V., Javornik, U., Plavec, J., Podgornik, A. and Rečnik, A. (2016) Self-assembly of multilevel branched rutile-type TiO_2 structures via oriented lateral and twin attachment. *Scientific Reports*, **6**, 24216.

21. Samriti, Prateek, Joshi, M. C., Gupta, R. K. and Prakash, J. (2022) Hydrothermal synthesis and Ta doping of TiO_2 nanorods: Effect of soaking time and doping on optical and charge transfer properties for enhanced SERS activity. *Materials Chemistry and Physics*, **278**, 125642.

22. Manojkumar, P., et al. (2022) Development of immobilised sunlight active W-Mo/Mo-V/V-W co-doped TiO_2 photocatalyst by plasma electrolytic oxidation. *Journal of Alloys and Compounds*, **919**, 165781.

23. Khanna, S., et al. (2021) Unravelling camphor mediated synthesis of TiO_2 nanorods over shape memory alloy for efficient energy harvesting. *Applied Surface Science*, **541**, 148489.

24. Chen, K., et al. (2021) Down-conversion Ce-doped TiO_2 nanorod arrays and commercial available carbon based perovskite solar cells: Improved performance and UV photostability. *International Journal of Hydrogen Energy*, **46**, 5677–5688.

25. Matouk, Z., Islam, M., Gutiérrez, M., Pireaux, J. J. and Achour, A. (2022) X-ray Photoelectron Spectroscopy (XPS) Analysis of Ultrafine Au Nanoparticles Supported over Reactively Sputtered TiO_2 Films. *Nanomaterials*, **12**, 20.

26. Tian, S., Liu, Q., Sun, J., Zhu, M., Wu, S. and Zhao, X. (2019) Mesoporous ZnO nanorods array with a controllable area density for enhanced photocatalytic properties. *Journal of Colloid and Interface Science*, **534**, 389–398.

27. Musa, M. Z., et al. (2022) Recent Progress on Titanium Dioxide-Based Humidity Sensor: Structural Modification, Doping, and Composite Approach. *Enabling Industry 4.0 through Advances in Manufacturing and Materials*, 507–516.